

UC San Diego

UC San Diego Previously Published Works

Title

Multifocal Calcifying Fibrous Tumor at Seven Intrathoracic Sites in One Patient

Permalink

<https://escholarship.org/uc/item/4b48491g>

Journal

The Annals of Thoracic Surgery, 111(2)

ISSN

0003-4975

Authors

Hernandez, Moises
Lin, Grace
Zhang, Yu
[et al.](#)

Publication Date

2021-02-01

DOI

10.1016/j.athoracsur.2020.05.100

Peer reviewed



Published in final edited form as:

Ann Thorac Surg. 2021 February ; 111(2): e85–e88. doi:10.1016/j.athoracsur.2020.05.100.

MULTIFOCAL CALCIFYING FIBROUS TUMOR AT SEVEN INTRATHORACIC SITES IN ONE PATIENT

Moises Hernandez, M.D.¹, Grace Lin, M.D.-Ph.D.², Yu Zhang, M.D.-Ph.D.¹, Ataollah Rajabnejad, M.D.¹, Francesca Balistreri¹, Patricia Thistlethwaite, M.D.-Ph.D.¹

¹Division of Cardiothoracic Surgery, University of California, San Diego 9300 Campus Point Drive La Jolla, CA 92037-7892

²Department of Pathology, University of California, San Diego 9300 Campus Point Drive La Jolla, CA 92037-7892

Abstract

Calcifying fibrous tumors (CFTs) are rare lesions that occur throughout the body. A 35-year-old man presented with exertional dyspnea. Computed tomography showed a polypoid mass abutting pericardium, diaphragm, and left chest wall, and a pleural-based lesion adjacent to T12. Thoracoscopy revealed a large mass with diaphragmatic stalk, two pleural-based nodules and four diaphragmatic nodules. Pathological analysis of resected lesions showed CFT. Three lesions contained heterogenous mutations associated with this tumor type. The patient is disease-free one-year later. CFTs should be recognized as rare multifocal pleural and diaphragmatic-based tumors. Complete resection leads to excellent survival for patients with this uncommon disease.

Keywords

Diaphragm; Thoracoscopy/VATS; Genetics/Genomics

Calcifying fibrous tumors (CFTs) are rare benign lesions that present as solitary or multifocal lesions in multiple locations in the body. Although mostly diagnosed in childhood, these tumors are also seen in young and middle-age adults. The majority of CFTs arise from the gastrointestinal tract, pleura, neck, mesentery, mediastinum, peritoneum, and thigh¹. 5.7% of these tumors present as synchronous lesions at diffuse sites². An extremely rare case of seven CFTs arising from diaphragm and pleura in a hemithorax of one patient is presented.

A 35-year-old man was referred for surgical evaluation of a calcified, multi-lobulated mass in the left chest. The patient was a long-distance cyclist, who developed exertional dyspnea and intermittent left lateral chest wall pain. Chest computed tomography (CT) showed a

Address Correspondence to: Patricia A. Thistlethwaite M.D.-Ph.D., 9300 Campus Point Drive, La Jolla, CA 92037-7892, pthistlethwaite@health.ucsd.edu.

Publisher's Disclaimer: This is a PDF file of an unedited manuscript that has been accepted for publication. As a service to our customers we are providing this early version of the manuscript. The manuscript will undergo copyediting, typesetting, and review of the resulting proof before it is published in its final form. Please note that during the production process errors may be discovered which could affect the content, and all legal disclaimers that apply to the journal pertain.

12.9×15.7 cm lobulated mass abutting the left pericardium, left lateral pleura and diaphragm (Fig. 1a), as well as a 4.7×0.9 cm pleural-based lesion adjacent to the T12 vertebral body (Fig. 1b). CT-guided biopsy of the larger mass was unsuccessful, due to inability of core biopsy needle to penetrate the mass, despite forceful pushing by the interventional radiologist. ¹⁸F-fluorodeoxyglucose positron emission tomography with CT (FDG-PET/CT) imaging revealed that both lesions had a maximum standardized uptake (SUV_{max}) of less than 1.2. The patient underwent video-assisted thoracoscopic resection. At operation, a large bone-like multi-lobulated mass was found to be connected to the dome of the diaphragm by a single adhesion and a vascularized stalk (Fig. 2a,b), which was resected with 2 cm of underlying diaphragm. The mass had no adhesions to pericardium, lung, or chest wall. There were two adjacent 2×0.9 cm fusiform nodules that were resected with underlying pleura next to the T12 (Fig. 2c). Visual examination of the hemithorax also revealed four subcentimeter tumorlets on the diaphragm, which were resected (Fig. 2c).

Pathological analysis of all seven lesions showed well-circumscribed, paucicellular, bland spindle cell tumors with abundant dense hyalinized collagen with areas of calcification (Fig. 3a-c), and focal lymphoplasmacytic infiltrate (Fig. 3b). No significant atypia, mitotic activity, or necrosis was identified.

Trichrome staining highlighted dense fibrotic stroma (Fig. 3d). By immunohistochemical staining, spindle cells were positive for vimentin, but negative for pankeratin, CK5–6, CK7, STAT6, ALK, and desmin, consistent with the diagnosis of CFT. Whole exome sequencing did not detect *ALK* gene mutation. The large mass demonstrated three de novo heterozygotic somatic mutations in exon 5 of the *Zinc Finger Protein 717* gene (*ZNF717*) on chromosome 3p12.3: 1) nucleotide 75786211: amino acid 855, serine > proline, 2) nucleotide 75786354: amino acid 807, threonine > isoleucine, 3) nucleotide 75787174: amino acid 534, proline > threonine. In contrast, the two nodules adjacent to T12 showed a single de novo heterozygotic somatic mutation in exon 7 of the *Facioscapulohumeral muscular dystrophy-1* gene (*FRG1*) on chromosome 4q35.2: nucleotide 190883080: amino acid 245, leucine > methionine, without mutation in the *ZNF717* gene.

The patient underwent repeat chest CT scanning at one year postoperatively, which demonstrated no evidence of recurrent disease.

COMMENT

Since the first description of CFTs in 1988³, the incidence of intrathoracic multifocal CFTs in the literature has been limited to less than 15 case reports. Within the chest, the most common location for CFTs is the parietal pleura, with lesions showing a predilection for the peribasilar or diaphragmatic pleural surface⁴. CFTs have also been reported in the mediastinum and lung parenchyma⁵. The median age for intrathoracic cases in the literature is 36 years, with a range of 22–59 years. 60% of pleural CFTs occur in females⁴.

CFT has been described in the World Health Organization Classification as a benign mesenchymal tumor. However, recently the molecular profile of CFTs has been examined,

in order to define possible driver mutations. Deleterious tumor-specific variants comprising heterozygotic de novo mutations have been identified in *ZNF717*, *Cell Division Cycle 27* (*CDC27*), and *FRG1* genes in CFTs⁶. These non-synonymous mutations produce altered proteins that may promote growth of CFTs. *ZNF717* contains a *Kruppel Associated Box* (*KRAB*) sequence seen in transcriptional regulatory genes controlling cellular proliferation, differentiation, and apoptosis. *FRG1* is a gene whose peptide levels are correlated with growth rates of prostate, lung, and colon carcinomas. In addition, whole exome sequencing has revealed tumor-specific copy number losses among most CFTs, on chromosome 6p22.2⁶.

It is interesting to note that in our patient, there were different mutations in the largest CFT and two of the six smaller CFT nodules resected. This may either represent the independent multifocal nature of these tumors or mutation resulting in clonal expansion and dissemination. Recently, Massoth et al.⁷ reported a case where tumor was present in contiguous visceral and parietal pleural adhesions near several pleural-based CFTs. Tumor within adhesions was speculated to represent a mode of dissemination or arborization across the pleural surfaces, leading to new areas of disease. In contrast, adhesions between visceral and parietal pleura were not seen in our case, and each resected tumor had a negative pleural or diaphragmatic margin.

The differential diagnosis of pleural and diaphragmatic CFTs includes inflammatory myofibroblastic tumors (IMFT), solitary fibrous tumors, sarcomatoid and desmoplastic mesothelioma, desmoid fibromatosis, leiomyoma, chronic fibrous pleuritis, and IgG4-related sclerosing disease. CFTs show lower cellularity, dense hyalinized stroma, and lack of *ALK* gene mutations, compared to IMFTs. Unlike CFTs, solitary fibrous tumors have a “pattern-less pattern”, *STAT6* immunoreactivity, and *NAB-STAT6* gene fusions. Sarcomatoid and desmoplastic mesothelioma may show malignant features and immunoreactivity for pankeratin, CK7, or mesothelial markers (e.g. FK5/6, calretinin), which are negative in CFTs. In contrast to CFTs, desmoid fibromatosis shows infiltrative growth and positive immunostaining for Beta-catenin. Leiomyomas immunostain positive for desmin, which is negative in CFTs. Chronic fibrosing pleuritis may be distinguished from CFTs by patient history of pleuritic chest pain, with pathological analysis showing diffuse or rind-like growth and inflammation. Although both CFTs and IgG4-related sclerosing disease show fibrosclerosis and lymphoplasmacytic infiltrate, IgG4-related sclerosing disease has more inflammation, many IgG4-positive plasma cells, and obliterative phlebitis.

The treatment of choice for multi-focal CFTs is complete surgical resection with negative intraoperative margins, along with careful examination of the hemithorax to remove all lesions. In our case, four diaphragmatic lesions were too small to be found by CT scanning and were identified and resected during thoracoscopy. Needle biopsy is often non-diagnostic, due to the calcified nature of these tumors and inability to penetrate them. Local recurrence rates after resection of pleural CFTs are up to 10% in the literature, occurring in the setting of incomplete resection^{2,8}. For patients who have undergone complete resection, we recommend a follow-up chest CT in one year, followed by surveillance chest CT scanning every five years thereafter. Long-term follow-up and a larger number of patients with CFTs is needed for a better understanding of this disease as it manifests in the chest.

Funding:

NIH R01 HL119543, NIH R01 HL132225

REFERENCES

1. Zhou J, Zhou L, Wu S, et al. Clinicopathologic study of calcifying fibrous tumor emphasizing different anatomical distribution and favorable prognosis. *Biomed Res Int*. 2019. 10.1155/2019/5026860.
2. Chorti A, Papavramidis TS, Michalopoulos A. Calcifying fibrous tumor: Review of 157 patients reported in international literature. *Medicine*. 2016;95:1–12.
3. Rosenthal NS, Abdul-Karim FW. Childhood fibrous tumor with psammoma bodies. Clinicopathologic features in two cases. *Arch Pathol Lab Med*. 1988;112:798–800. [PubMed: 3395217]
4. Mazi A, Emil S, Bernard C, et al. Symptomatic calcifying fibrous tumor of the pleura in a teenager. *J Pediatr Surg Case Rep*. 2018;30:34–7.
5. Dissanayake SN, Hagen J, Fedenko A, et al. Calcifying fibrous pseudotumor of the posterior mediastinum with encapsulation of the thoracic duct. *Ann Thorac Surg*. 2016;102:e39–40. [PubMed: 27343527]
6. Mehrad M, La Framboise WA, Lyons MA, et al. Whole-exome sequencing identifies unique mutations and copy number losses in calcifying fibrous tumor of the pleura: report of 3 cases and review of the literature. *Hum Pathol*. 2018;78:36–43. [PubMed: 29689243]
7. Massoth LR, Selig MK, Little BP et al. Multiple calcifying fibrous pseudotumors of the pleura: ultrastructural analysis provides insight on mechanism of dissemination. *Ultrastruct Pathol*. 2019;43:154–161. [PubMed: 31746679]
8. Shibata K, Yuki D, Sakata K. Multiple calcifying fibrous pseudotumors disseminated in the pleura. *Ann Thorac Surg*. 2008;85:e3–5. [PubMed: 18222223]

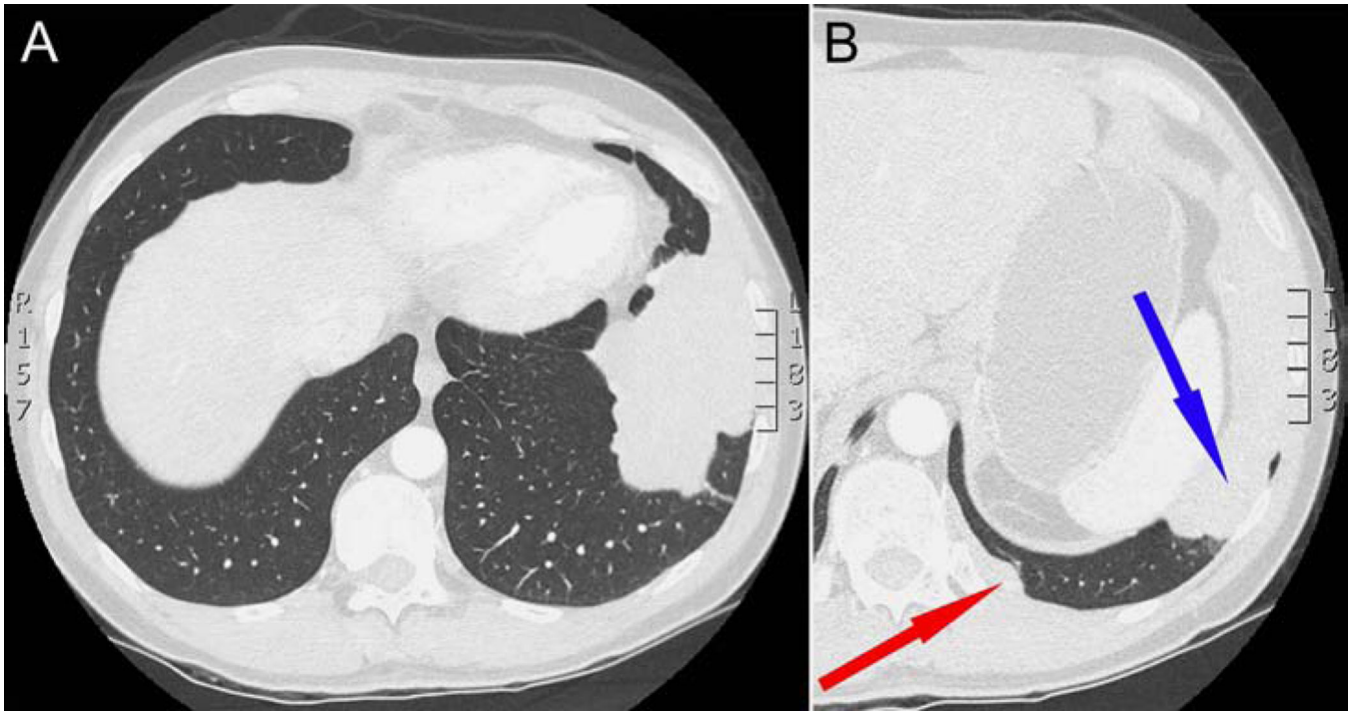


Figure 1.

(A) CT imaging showing a large multi-lobulated mass abutting the lateral chest wall, diaphragm, and pericardium, and (B) a smaller lesion adjacent to the T12 vertebral body (red arrow), with large mass seen in (A) (blue arrow).

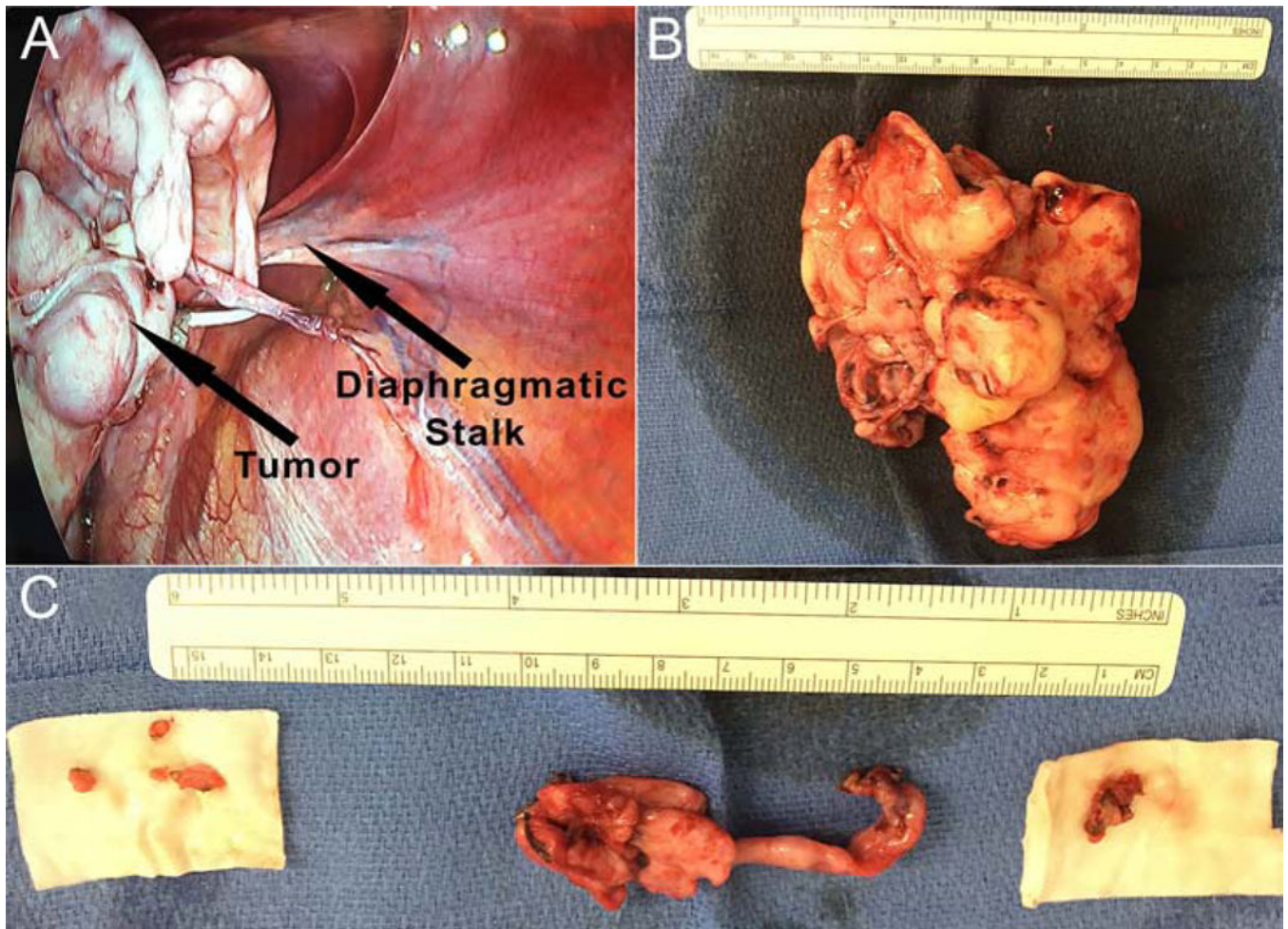


Figure 2. (A) Video-assisted thoracoscopic intraoperative view of the large multi-lobulated mass with single stalk to the diaphragm. (B) resected large multi-lobulated calcified mass, (C) two resected contiguous, but separate nodules overlying the T12 vertebral body (middle tumors in image) and four resected tumorlets from the diaphragm (right and left tumors in image).

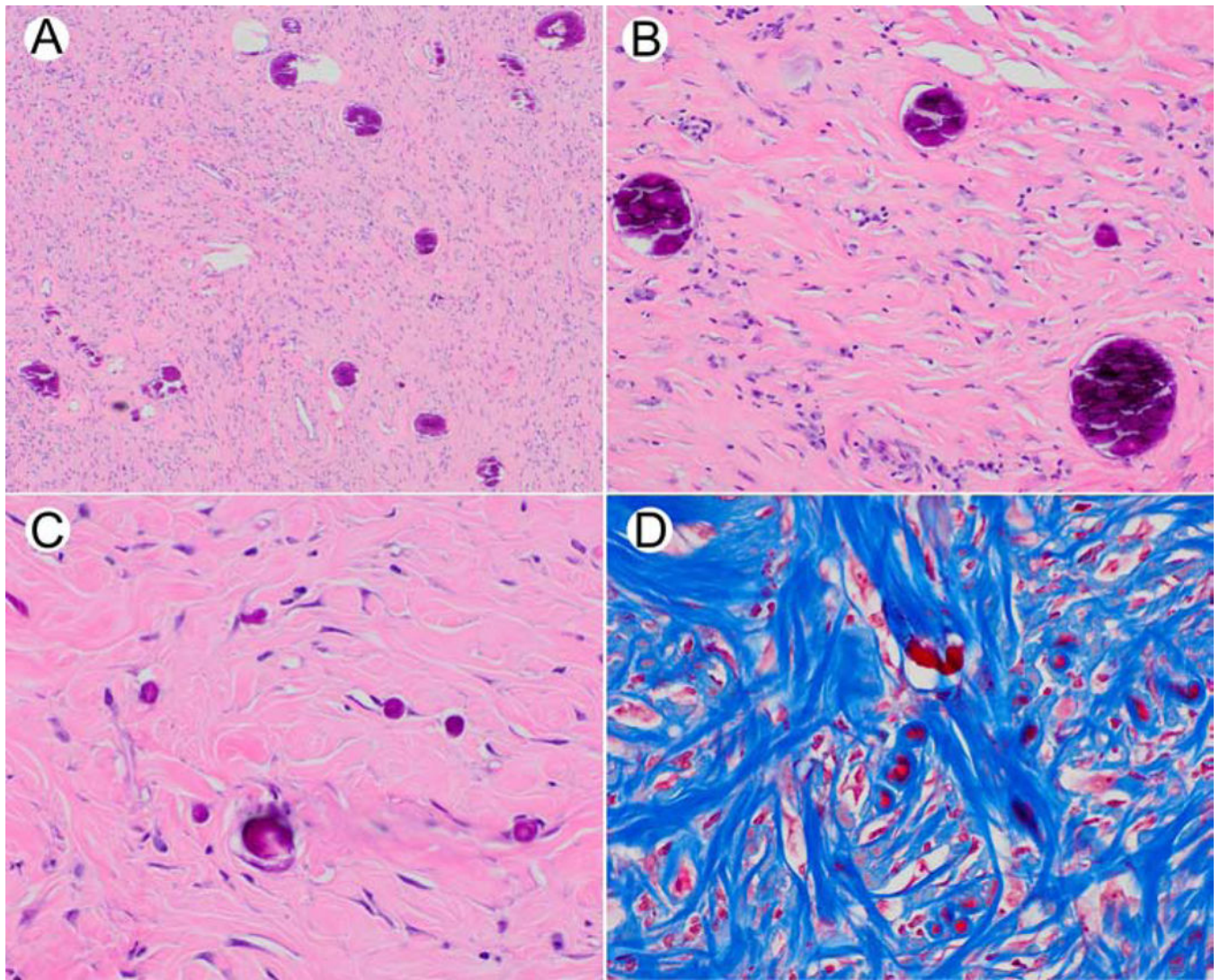


Figure 3. Microscopic features of the largest mass shows bland spindle cells, densely hyalinized collagen in storiform and whorled arrangement, psammomatous calcifications, and patchy lymphoplasmacytic infiltrates. Hematoxylin and eosin stain, (40X, A) (200X, B) (400X, C). (D) Trichrome staining of dense fibrotic stroma in the largest mass (magnification 400X).